Contents lists available at ScienceDirect

Applied Clay Science

Research paper

Strengthening and stiffening carbon fiber epoxy composites by halloysite nanotubes, carbon nanotubes and silicon carbide whiskers

Seungjin Han, D.D.L. Chung *

Composite Materials Research Laboratory, University at Buffalo, State University of New York, Buffalo, NY 14260-4400, USA

ARTICLE INFO

ABSTRACT

Low-cost natural halloysite (Hal) nanotubes (0.1 μm diameter) were effective for strengthening and stiffening continuous fiber epoxy composites, as shown for cross-ply carbon fiber (5 μm diameter, ~59 vol.%) epoxy nanocomposites under flexure, giving 17% increase in strength, 11% increase in modulus and 21% decrease in ductility. They were less effective than expensive multiwalled carbon nanotubes (0.02 μm diameter), which gave 25% increase in strength, 11% increase in modulus and 14% decrease in ductility. However, they were more effective than expensive silicon carbide whiskers (1 μm diameter), which gave 15% increase in strength, 9% increase in modulus and 20% decrease in ductility. Each filler, at ~2 vol.%, was incorporated in the composite at every interlaminar interface (interface between adjacent fiber laminae) by fiber prepreg surface modification. The flexural strength increase due to Hal nanotubes incorporation corroborated with the interlaminar shear strength increase. The measured values of the composite modulus agreed roughly with the calculated values based on the Rule of Mixtures. The interlaminar interface thickness was higher for the SiC whiskers case than the carbon nanotubes or Hal nanotubes case. The lamina thickness was not affected by the fillers. The composite density was 2% higher for the Hal nanotubes and SiC whiskers cases than the carbon nanotubes case.

© 2013 Elsevier B.V. All rights reserved.

1. Introduction

Continuous carbon fiber polymer composites are important lightweight structural materials due to their combination of high elastic modulus, high strength and low density. Lightweight structures using these composites include aircrafts, automobiles, bicycles, ships, wind turbines, bridge decks, offshore platforms, sporting goods, etc.

Continuous carbon fibers are more effective as primary reinforcements than discontinuous carbon fibers, carbon nanofibers and carbon nanotubes, because of the continuous length, good alignment and the consequent high maximum volume fraction of continuous fibers in a composite. However, the discontinuous reinforcement may be used as a secondary reinforcement in composites that involve continuous carbon fibers as the primary reinforcement. Throughout this paper, fiber refers to continuous fiber.

Because the continuous fibers render high modulus and strength to the composite anyway, the stiffening and strengthening of continuous fiber composites are more challenging than those of composites without continuous fibers. For structural performance, high values of both modulus and strength are necessary. Furthermore, stiffening without strengthening tends to cause decrease in the ductility. Thus, simultaneous stiffening and strengthening are desired.

Considerable prior work that incorporated carbon nanotubes in continuous fiber polymer composites had been reported. Increases in the interlaminar shear strength (the maximum shear stress that can be borne by the interlaminar interface, which is the interface between adjacent laminae, where a lamina refers to a ply of fibers) (Godara et al., 2010; Gojny et al., 2005; Zhu et al., 2007), high-cycle fatigue life (Grimmer and Dharan, 2008) and delamination (local separation of adjacent laminae) fatigue resistance (Grimmer and Dharan, 2010) in glass fiber composites were achieved. In addition, the carbon nanotubes provided electrical conductivity to the glass fiber composite, thus rendering the composite the ability to sense strain and damage through electrical resistance measurement (Alexopoulos et al., 2010; Gao et al., 2009; Rausch and Mader, 2010; Sureeyatanapas and Young, 2009; Thostenson et al., 2009; Zhang et al., 2010) and the ability to shield electromagnetic radiation (Lee et al., 2011). Increases in the interlaminar shear strength (Bekyarova et al., 2007; Cho and Daniel, 2008; F. Zhang et al., 2009; X. Zhang et al., 2009), compressive strength (Cho and Daniel, 2008; Cho et al., 2008), flexural strength and modulus (Kim et al., 2009), fiber–matrix interfacial load transfer effectiveness (Thostenson et al., 2002) and the storage modulus (under dynamic flexure at 1 Hz, increased by 75%) (Kar et al., 2009) were achieved similarly in carbon fiber polymer composites. In spite of the increase in the interlaminar shear strength and flexural strength and modulus, the tensile modulus and strength of carbon fiber epoxy composites were not affected by the incorporation of MWCNT (multiwalled carbon nanotubes) (Bekyarova et al., 2007) or a mixture of CNT (carbon nanotubes) with 1, 2 and 3 walls (Kim et al., 2009), because the tensile properties were dominated by the continuous fibers.

* Corresponding author. Tel.: +1 716 645 3977; fax: +1 716 645 2883.
E-mail address: ddlchung@buffalo.edu (D.D.L. Chung).

Various methods were used in prior work to incorporate CNT in continuous fiber polymer nanocomposites. These methods included dispersing the nanotubes in the fiber sizing or coating (Godara et al., 2010; Rausch and Mader, 2010; Sureeyatanapas and Young, 2009; Zhang et al., 2010), dispersing the nanotubes in the matrix (Gao et al., 2009; Godara et al., 2010; Grimmer and Dharan, 2008, 2010; Thostenson et al., 2009), applying the nanotubes to the fiber surface or the fiber fabric surface by electrophoretic deposition (Bekyarova et al., 2007; Zhang et al., 2010), and grafting the nanotubes onto the fiber surface by chemical vapor deposition (Kar et al., 2009; Thostenson et al., 2002; F. Zhang et al., 2009).

Much less research was reported on the incorporation of fillers other than carbon nanotubes in continuous fiber polymer composites, in spite of the relatively low cost of other fillers. The incorporation of halloysite (Hal) nanotubes (a natural clay mineral, Brigatti et al., 2006) in the matrix of woven carbon fiber epoxy nanocomposites increased the flexural strength by 14% and the interlaminar shear strength by up to 25%, while the flexural modulus was essentially unaffected (Ye et al., 2011a,b). The incorporation of silicon carbide whiskers at the interlaminar interface of unidirectional carbon fiber composites by spraying the whiskers on the prepreg surface improved the interlaminar fracture toughness, though the strength and modulus were not reported (Wang et al., 2002). The incorporation of montmorillonite (Mt) in the carbon fiber epoxy nanocomposites increased the flexural strength and modulus by 31% and 46% respectively (Chowdhury et al., 2007). Mt was not as effective as alumina particles for increasing the interlaminar shear strength or the transverse flexural strength (Timmerman et al., 2002). The incorporation of alumina particles (25 nm) in carbon fiber epoxy nanocomposites made by filament winding increased the flexural toughness and interlaminar shear strength (Hussain et al., 1996). The incorporation of 48-μm Al_2O_3 particles in the epoxy matrix of a woven continuous glass fiber composite resulted in 78% increase in flexural modulus and 33% increase in the flexural strength (Asi, 2009). The incorporation of 20–30 nm silica particles to the epoxy matrix of a glass fiber fabric composite increased the interlaminar fracture toughness and the impact resistance (Uddin and Sun, 2008).

Relatively little research was reported on the incorporation of carbon fillers other than carbon nanotubes in continuous fiber polymer composites, in spite of the relatively low cost of these other fillers, such as carbon black and carbon nanofiber. By using carbon black as a filler located at the interlaminar interface of a continuous carbon fiber epoxy composite, the flexural modulus was increased by 6.4% and 11% for unidirectional and cross-ply composites respectively (Han et al., 2008). By incorporating carbon nanofibers (originally known as carbon filaments) in the epoxy matrix of a woven continuous carbon fiber nanocomposite, the flexural strength was increased by 22% while the tensile strength was increased by 11% (Zhou et al., 2006, 2008). However, by using 0.1-μm diameter carbon nanofibers as an interlaminar filler (a filler located at the interlaminar interface) in a continuous carbon fiber epoxy nanocomposite, the tensile modulus and the dynamic flexural modulus were decreased (Hudnut and Chung, 1995; Segiet and Chung, 2000).

The effects of a filler in the absence of continuous fibers (Du et al., 2010; He et al., 2012; Jia et al., 2011; Kong et al., 2011; Lecouvet et al., 2011; Rooj et al., 2011) received more attention than those in the presence of continuous fibers. In spite of the prior work mentioned above on the effects of various fillers in the presence of continuous fibers, comparative evaluation of competing fillers received little or no attention.

The objectives of this paper are (i) to provide a cost-effective method of strengthening and stiffening continuous carbon fiber polymer composites, (ii) to investigate the effectiveness of Hal nanotubes incorporation for strengthening and stiffening carbon fiber polymer composites, (iii) to compare the effects of various high-elastic-modulus fillers, namely an expensive nanofiller (carbon nanotubes), an inexpensive nanofiller (Hal nanotubes) and a microfiller (silicon carbide whiskers

of diameter 1 μm, chosen due to their effectiveness for strengthening polymers (Li and Chung, 1994), aluminum (Lai and Chung, 1996), copper (Yih and Chung, 1996), brass (Yih and Chung, 1999) and silicon nitride (Wang and Chung, 1997)), on the mechanical properties of the composites, and (iv) to correlate the structure and the mechanical properties of these composites.

2. Experimental methods

2.1. Materials

Composite specimens were fabricated by hand lay-up and compression molding of a stack of cross-ply carbon fiber epoxy prepreg sheets. The curing conditions were 90 min at 177 °C and a pressure of 0.5 MPa, unless noted otherwise.

Unless noted otherwise, the carbon fiber prepreg had RS-36 epoxy, with uncured resin density 1.20–1.25 g/cm^3, resin content (33 ± 2) wt.%, uncured prepreg density 1.394 ± 0.006 g/cm^3 (measured in this work) and fiber volume fraction (obtained from the uncured prepreg density, based on the Rule of Mixtures, i.e., a method of estimating composite properties based on the averaged properties of the components) 0.274 ± 0.010. The prepreg was manufactured by Tencate Advanced Composites USA, Inc., Morgan Hill, CA. Unless noted otherwise, the carbon fibers had designation Torayca M46JB, in the form of 12 K PAN-based fibers, with tensile modulus 436 GPa, tensile strength 4.0 GPa, fiber diameter 5.0 ± 0.3 μm (measured in this work), and elongation at break 1.0%.

For the short-beam shear testing only, the carbon fiber prepreg was from Tencate Advanced Composites USA, Inc., with the carbon fibers designated Pyrofil TR50S 15 K (with diameter 7 μm, density 1.82 g/m^3, tensile modulus 235 GPa, tensile strength 4.9 GPa and elongation at break 2.1%) and with TC275 epoxy; the resin content of the prepreg was 34 ± 2 %. Curing was conducted at 177 °C and 0.1 MPa for 120 min.

Specimens with and without modification were prepared for comparative evaluation. Two lay-up configurations were studied, namely unidirectional and cross-ply configurations. The cross-ply configuration was symmetrical around the central 90° lamina.

The fillers were MWCNT, silicon carbide whiskers and Hal nanotubes. Unless stated otherwise, the MWCNT was from Nanothinx S.A., Greece, NTX1, with 15–35 nm diameter, 15–35 layers, ≥10 μm length, 97% nanotubes purity, 3% metal particles, <1% amorphous carbon, and 1.4 g/cm^3 density. For the short-beam shear testing specimens only, the MWCNT was from ILJIN, S. Korea, as prepared by chemical vapor deposition, with purity above 95%, length exceeding 60 μm, average diameter 50 nm and density 1.4 g/cm^3. The silicon carbide whiskers (abbreviated SiCw) had a cubic crystal structure, with 1.4 μm mean diameter, 18.6 μm mean length, 99 wt.% SiC, 0.4 wt.% SiO_2 and density 3.21 g/cm^3, provided by Advanced Refractory Technologies, Inc., Buffalo, NY. The Hal nanotubes were in the form of natural hollow tubes, as provided by NaturalNano, Inc., Rochester, NY. They were heated by NaturalNano at 600 °C (abbreviated HHal). Based on powder x-ray diffraction patterns obtained using CuKα radiation and a Siemens Kristalloflex diffractometer (Fig. 1), HHal was highly disordered, with a basal spacing of 7 Å, indicating that it was unhydrated Hal (Huertas et al., 2004; Wada, 1965). The diameter and length of HHal were roughly 0.1–0.2 and 0.4–0.5 μm respectively, as shown by scanning electron microscopy (Fig. 2); the density was 2.53 g/cm^3.

The interlaminar interface modification was performed by wet application of the filler on both opposite surfaces of a prepreg sheet. During the wet application, the filler was dispersed in a solvent at a solid content that was low enough for good workability (spreadability) of the dispersion. The content of 2 mass % was used for HHal and SiCw dispersions and the content of 0.8 mass % was used for the MWCNT dispersion. Higher contents were not used in order to maintain low viscosity for effective application on the prepreg surface. Thus, the
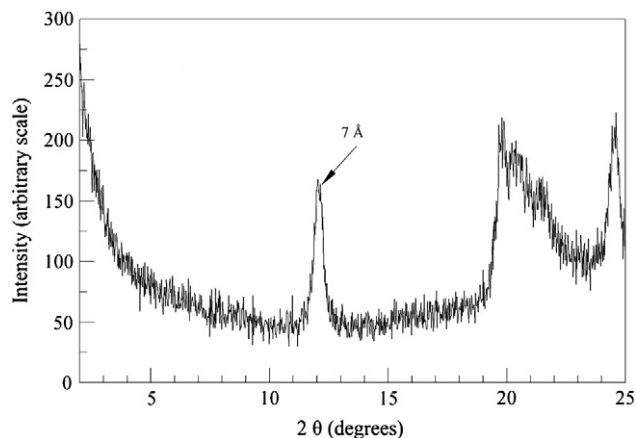
Fig. 1. X-ray diffraction pattern of Hal nanotubes (HHal). The arrow indicates the 001 reflection indicating a basal spacing of 7 Å.

different fillers were used at different contents, such that the contents used gave similar workability of the filler dispersion.

The solvent was such that it could evaporate at room temperature within a day after application of the dispersion on a prepreg sheet by immersion. The ethylene glycol monoethyl ether (EGME) solvent (Han et al., 2008) dissolved a part of the excessive resin on the surface of the prepreg, so that the thickness of the interlaminar interface region of the resulting composite was kept close to that of the unmodified composite. After solvent evaporation, 15 prepreg sheets were stacked, thus resulting in 14 interlaminar interfaces. In the unmodified composite, none of the 14 interlaminar interfaces was modified. In a modified composite, all of the 14 interlaminar interfaces were modified. The curing conditions (time, temperature and pressure) were essentially those recommended by the prepreg manufacturer (90 min, 177 °C and 0.5 MPa).

2.2. Density measurement

The density was derived from the mass and dimensions of 15-lamina composite specimens of size 15 × 11 × 2.0 mm. The composite thickness of each type of composite was determined by a micrometer, with the measurement performed for 5 (or more) specimens. Three specimens of each type were measured in terms of the density.

The composite density was used to obtain the fiber volume fraction, based on the Rule of Mixtures. For this purpose, the densities of the fiber and matrix were needed. According to Tencate, the densities of the

Fig. 2. SEM image of Hal nanotubes (HHal).

carbon fiber and epoxy matrix in the carbon fiber prepreg were 1.84 and 1.23 g/cm³ respectively.

2.3. Flexural testing

Mechanical testing was performed on 15-lamina specimens under three-point bending up to failure, using a hydraulic mechanical testing system (MTS Systems Corp., Eden Prairie, MN). The specimen size was 80 × 11 × 2.0 mm. The span was 58 mm. The flexural strength was the highest stress prior to failure (not necessarily the first abrupt decrease in stress in the stress–strain curve). The flexural modulus was obtained from the slope of the straight-line portion of the curve of flexural stress vs. flexural strain. This portion constituted most of each curve. The flexural ductility was the strain at failure, which was the last abrupt drop in stress in the stress–strain curve. Other than the unmodified cross-ply carbon fiber composite, only one abrupt drop in stress occurred en route to failure. At least four specimens of each composition were tested.

2.4. Short-beam shear strength testing

Cross-ply composite specimens with 33 laminae, fabricated at a curing pressure of 0.1 MPa and of size 35 × 15 × 4.3 mm were tested for the short beam shear (SBS) strength, i.e., the interlaminar shear strength. The test was conducted under flexure at a span of 20 mm and a span-to-thickness ratio of 4.7:1. Six specimens of each type were tested.

The SBS strength (F) was calculated using the equation

$$F = 0.75 \frac{P}{bd} \tag{1}$$

where P is the force at the composite failure load, b is the specimen width (15 mm), and d is the specimen thickness (4.3 mm).

2.5. Microscopy

Optical microscopy was conducted at the mechanically polished edge of each composite, i.e., the surface perpendicular to the plane of the laminate. The interlaminar interface thickness and lamina thickness were thus measured. The former was determined by measurement at 10 points located at various interlaminar interfaces in the composite. The latter was determined by measurement at 5 (or more) points located at various laminae in the composite.

3. Results and discussion

3.1. Composite density, constituent volume fractions and composite architecture

Based on the measured density of the unmodified and modified composites (Table 1), the Rule of Mixtures and the measured mass and known density of the filler incorporated, the volume fractions of the carbon fiber, matrix and filler were obtained (Table 1).

The volume fraction of the filler was small, ranging from 0.014 to 0.024. The dominant constituent was the carbon fiber, which ranged in volume fraction from 0.579 to 0.599. Any of the fillers caused the fiber volume fraction to increase slightly and caused the matrix volume fraction to decrease slightly. This was partly due to the partial removal of the interlaminar resin during prepreg surface modification.

The density was increased slightly upon addition of the filler. The density for the cases of HHal and SiCw was 2% higher than that for the MWCNT case, due to the relatively high densities of HHal and SiCw.

The composite architecture is described in terms of the thicknesses of the laminae and of the interlaminar interfaces (Table 2). The
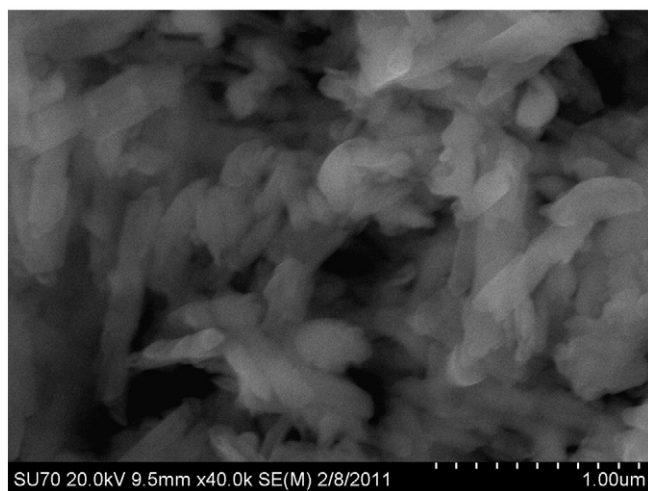
Table 1
Composite density and the volume fractions of the fiber, matrix and filler for cross-ply carbon fiber epoxy composites made at a curing pressure of 0.5 MPa with and without the filler.

Filler content[a]	Density of composite (g/cm³)	Volume fraction		
		Fiber[b]	Matrix[b]	Filler[c]
0%	1.583 ± 0.005	0.579 ± 0.020	0.421 ± 0.019	0
0.8% MWCNT	1.592 ± 0.001	0.586 ± 0.001	0.390 ± 0.003	0.024 ± 0.005
2% HHal	1.618 ± 0.007	0.599 ± 0.007	0.383 ± 0.004	0.017 ± 0.003
2% SiCw	1.620 ± 0.002	0.593 ± 0.006	0.393 ± 0.004	0.014 ± 0.002

[a] Fraction of mass of dispersion.
[b] Calculated from the measured density, based on the Rule of Mixtures.
[c] Obtained by dividing the volume of the filler by the volume of the composite, with the volume of the filler obtained by dividing the mass of the filler by the density of the filler. The mass of the filler was obtained by subtracting the mass of the prepreg that had been treated by the solvent in the absence of the filler from the mass of the prepreg that had been treated by the solvent in the presence of the filler.

composite thickness was due to these two contributions, i.e., the composite thickness was contributed by the thicknesses of the 14 interlaminar interfaces and those of the 15 laminae. The volume fraction of interlaminar interface was obtained by dividing the total thickness of all 14 interlaminar interfaces by the composite thickness.

The optical microscope photograph of the edge of a cross-ply unmodified (Fig. 3) or modified (Fig. 4) composite shows an interlaminar interface and parts of the two laminae proximate to it. The interface region was the region without fibers and located between adjacent laminae. Individual SiC whiskers were observed (Fig. 4(c)), though individual filler units were not observed for the other fillers. This was because of the relatively large diameter of the whiskers. Comparison of Figs. 3 and 4 showed that the filler caused the interlaminar interface thickness to change negligibly.

Table 2 lists the interlaminar interface thickness, lamina thickness, composite thickness and interlaminar interface volume fraction of unmodified and modified composites. The interlaminar interface thickness was below about 11 μm for all of the modified and unmodified composites, such that the thickness was slightly higher for the SiCw case than the MWCNT or HHal case. That the filler incorporation had little effect on the interlaminar interface thickness is consistent with the fact that a part of the excessive resin in the interface region had been removed by solvent dissolution during the process of filler incorporation. The relatively large thickness for the SiCw case is attributed to the relatively large diameter of the whisker. The lamina thickness and the composite thickness were essentially not affected by the filler incorporation. Hence, the interlaminar interface thickness appeared to be the main dimensional parameter that was affected by the filler, as expected.

The interlaminar interface volume fraction (Table 2) was less than about 7% for all of the modified and unmodified composites. It was highest when the filler was SiCw, due to the relatively high interlaminar interface thickness.

Table 2
Interlaminar interface thickness, lamina thickness, composite thickness, and interlaminar interface volume fraction of carbon fiber cross-ply epoxy composites fabricated at a curing pressure of 0.5 MPa with and without the interlaminar filler.

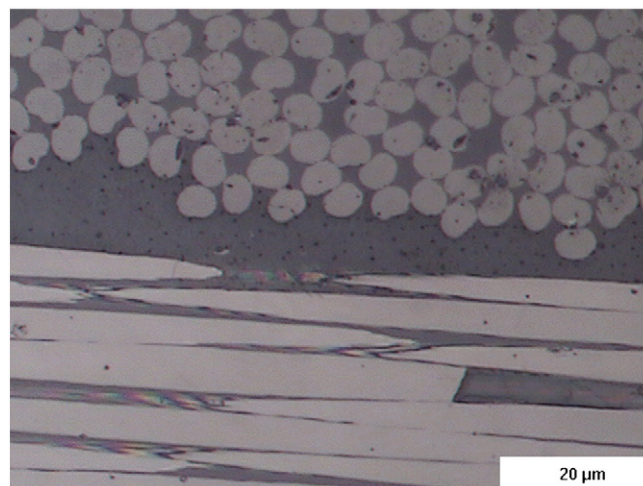| Filler content[a]	Interlaminar interface thickness (μm)	Lamina thickness (μm)	Composite thickness (μm)	Interlaminar interface volume fraction (%)
0%	8.1 ± 3.1	139.8 ± 6.8	2100 ± 75	5.4 ± 2.3
0.8% MWCNT	7.6 ± 3.1	139.4 ± 8.4	2132 ± 30	5.0 ± 2.8
2% HHal	7.5 ± 3.1	137.6 ± 7.9	2090 ± 50	5.0 ± 2.7
2% SiCw	10.5 ± 3.7	141.5 ± 8.1	2174 ± 54	6.7 ± 3.1

[a] Fraction of mass of dispersion.

Fig. 3. Optical microscope photograph of the edge of unmodified cross-ply carbon fiber epoxy composite (0.5 MPa curing pressure).

3.2. Flexural properties

For all the cross-ply composites, the curve of the flexural stress versus flexural strain during static three-point bending in the longitudinal direction up to failure (Fig. 5) was essentially a straight line up to the first abrupt drop in stress, which corresponded to the first major damage. Up to several abrupt drops in stress occurred in the route to failure. The occurrence of multiple abrupt drops in stress was probably due to the fracture of the 0° fibers of the surface lamina occurring not all at once.

Tables 3 and 4 show that the various types of filler differed in their effectiveness for stiffening and strengthening. The MWCNT (2.4 vol.%) was most effective, giving 11% increase in the modulus, 25% increase in the strength and 14% decrease in the ductility, such that the fractional changes in modulus and strength were relative to the unmodified composite having the same fiber volume fraction (since the fiber volume fraction differed between unmodified and modified composites). The HHal (1.7 vol.%) was almost as effective as MWCNT, giving 11% increase in the modulus and 17% increase in the strength, though the 21% decrease in the ductility was relatively high. The SiCw (1.4 vol.%) was slightly less effective than HHal, giving 9% increase in modulus, 15% increase in strength and 20% decrease in ductility. The finding that SiCw was less effective than HHal, in spite of their high reinforcing ability for other types of composite (Lai and Chung, 1996; Li and Chung, 1994; Yih and Chung, 1996, 1999), is attributed mainly to the relatively large diameter of SiCw and the consequent heterogeneity in the filler distribution in the interlaminar interface region (Fig. 4(c)).

Among the various types of filler, MWCNT was the most expensive, followed by SiCw. The HHal was much less expensive than both MWCNT and SiCw. Thus, with both cost and performance taken into consideration, HHal is particularly attractive.

Interlaminar fracture (Bazhenov, 1995) was observed for both modified and unmodified cross-ply composites. Fiber fracture was observed on the compression surface shortly before the occurrence of interlaminar fracture only for some of the specimens of cross-ply carbon fiber composites (both modified and unmodified). This fiber fracture resulted in a crack extending along the full width of the composite at the midspan position, as previously reported (Wang and Chung, 2006).

In practice, multidirectional composites such as quasi-isotropic composites are used for structural applications. Due to their transverse weakness, unidirectional composites are not used in practice. From a scientific viewpoint, cross-ply composites are akin to multidirectional composites, whereas unidirectional composites are much different.

a

b

c
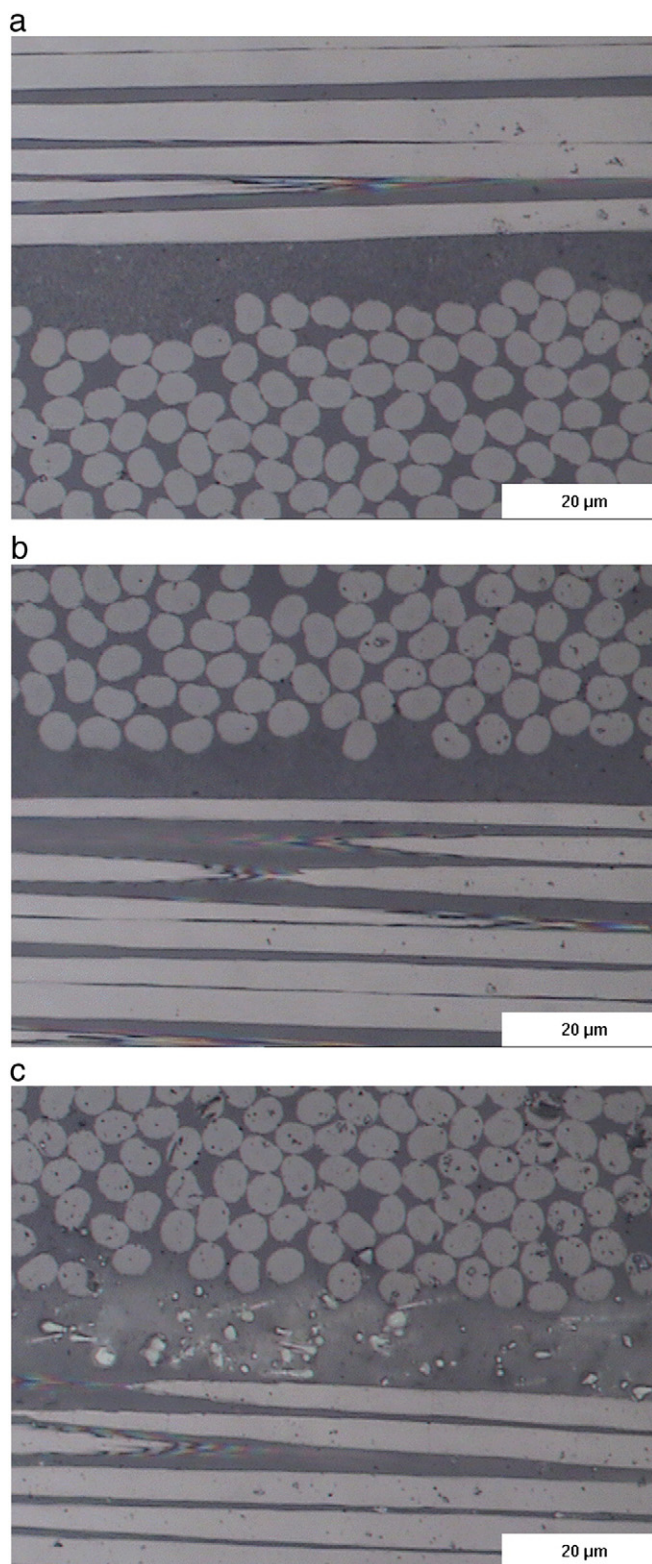
Fig. 4. Optical microscope photographs of the edge of modified cross-ply carbon fiber epoxy composites (0.5 MPa curing pressure). (a) 0.8% MWCNT. (b) 2% Hal nanotubes (HHal). (c) 2% silicon carbide whiskers (SiCw). The percentages refer to the fraction by mass of the filler in the dispersion used to apply the filler to the prepreg surface.

Therefore, the observed attractiveness of the cross-ply composites will likely also apply to multidirectional composites in general.

Unmodified unidirectional composites were tested along the longitudinal (0°) and transverse (90°) directions for the purpose of obtaining
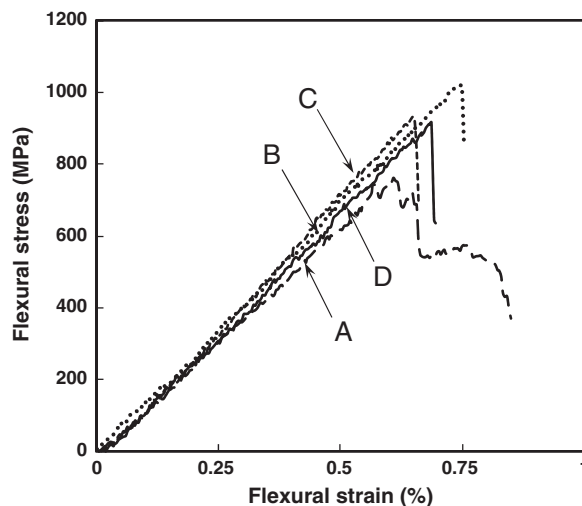
Fig. 5. Curves of flexural stress versus flexural strain during static flexure up to failure for modified and unmodified cross-ply carbon fiber epoxy composites (0.5 MPa curing pressure). A: No filler; B: 0.8 mass % MWCNT; C: 2 wt.% Hal nanotubes (HHal); D: 2 mass % silicon carbide whiskers (SiCw). The percentages refer to the fraction by mass of the filler in the dispersion used to apply the filler to the prepreg surface.

the effective fiber modulus in these two directions from the measured composite modulus values. The longitudinal and transverse composite modulus values were 214 ± 6 and 7.5 ± 1.0 GPa respectively; the longitudinal and transverse composite strength values were 1561 ± 30 and 59 ± 3 MPa respectively; the associated plots of flexural stress vs. flexural strain are shown in Fig. 6.

The fractional increases in flexural modulus and strength due to MWCNT incorporation (Table 4) were similar to those previously reported for woven carbon fiber epoxy nanocomposites with MWCNT incorporated in the matrix (Kim et al., 2009). The MWCNT content was 0.27 vol.% in prior work (Kim et al., 2009), compared to 2.4 vol.% in this work. This prior work (Kim et al., 2009) reported a fractional increase of ductility of 11% due to the MWCNT incorporation, in contrast to the fractional decrease of ductility of 14% obtained in this work. This large difference in the ductility effect was due to the fact that the

Table 3
Flexural modulus/strength/ductility and their fractional change due to the presence of the filler for cross-ply carbon fiber epoxy composites fabricated at a curing pressure of 0.5 MPa with and without the interlaminar filler.

Filler content[a]	Modulus (GPa)	Strength (MPa)	Ductility (%)
0%	123 ± 2	789 ± 17	0.85 ± 0.05
		774 ± 47[b]	0.65 ± 0.03[b]
0.8% MWCNT	138 ± 6 (124.5[c])	1002 ± 11 (799[c])	0.73 ± 0.02
2% HHal	141 ± 3 (127.2[c])	958 ± 72 (816[c])	0.67 ± 0.04
2% SiCw	137 ± 3 (126.0[c])	933 ± 51 (808[c])	0.68 ± 0.04
	Fractional change in modulus	Fractional change in strength	Fractional change in ductility
0.8% MWCNT	12% ± 6% (11% ± 6%[d])	27% ± 4% (25% ± 5%[d])	−14% ± 8%
2% HHal	15% ± 4% (11% ± 5%[d])	21% ± 12% (17% ± 12%[d])	−21% ± 10%
2% SiCw	11% ± 5% (9% ± 4%[d])	18% ± 9% (15% ± 9%[d])	−20% ± 10%

[a] Fraction of mass of dispersion.

[b] Values at the first abrupt decrease in stress, which differs from the point of failure only for the case of 0% filler.

[c] Calculated value of the unmodified composite, obtained by scaling the measured value of the unmodified composite to the value for the higher fiber volume (Table 1) of the modified composite.

[d] Fractional change relative to the calculated value obtained for the unmodified composite by scaling the measured value of the unmodified composite to the value for the higher fiber volume of the modified composite (Table 1).

Table 4
Short-beam shear strength of cross-ply carbon fiber epoxy composites with and without filler.

Filler content (fraction of mass of dispersion)	Strength (MPa)	Fractional change in strength relative to the case without filler
None	53.0 ± 1.6	/
0.8 wt.% MWCNT[a]	54.2 ± 1.6	+2% ± 6%
2 wt.% HHal	60.6 ± 4.9	+14% ± 13%
2% SiCw	50.5 ± 4.7	−5% ± 7%

[a] MWCNT, From ILJIN, S. Korea, as prepared by chemical vapor deposition, with purity higher than 95%, the length > 60 μm and average diameter 50 nm.

prior work (Kim et al., 2009) did not measure the ductility (with no ductility or strain data presented) but probably calculated the ductility from the measured strength and modulus by assuming that the stress–strain curve was a straight line up to failure. In contrast, this work measured the ductility. The fractional increases in flexural modulus and strength due to HHal incorporation (Table 4) were comparable to or higher than those of prior work (Ye et al., 2011a,b), which was for woven carbon fiber epoxy nanocomposites with Hal nanotubes (presumably without heat treatment) incorporated in the matrix. The fractional

Fig. 6. Curves of flexural stress versus flexural strain during static flexure up to failure for the unmodified unidirectional carbon fiber epoxy composites (0.5 MPa curing pressure). (a) 0° composite. (b) 90° composite.

increases in Table 4 were lower than those previously reported for woven carbon fiber epoxy–matrix nanocomposites with Mt incorporated in the matrix (Kar et al., 2009) or woven glass fiber epoxy composites with Al_2O_3 particles incorporated in the matrix (Asi, 2009). The difference in the results of this work compared to those of prior work (Kim et al., 2009) was due to (i) the filler being incorporated in the matrix in prior work (Asi, 2009; Kim et al., 2009; Wang et al., 2002; Ye et al., 2011a,b), whereas it was incorporated at the interlaminar interface in this work, and (ii) the woven nature of the continuous fibers in the prior work (Asi, 2009; Kim et al., 2009; Wang et al., 2002; Ye et al., 2011a,b), and the consequent spaces within the fabric for occupation by the filler.

3.3. Short-beam shear strength

The short-beam shear strength (interlaminar shear strength) was increased by the addition of HHal (Table 4). The fractional increase was greater than that of prior work (Ye et al., 2011a) for woven carbon fiber epoxy composite with Hal nanotubes (presumably without heat-treatment). This strength was essentially unaffected by the addition of MWCNT or SiC whisker (Table 4). This was probably due to the very small length of HHal compared to MWCNT or SiC whisker. A smaller length increases the likelihood for the filler to stand up in a direction roughly perpendicular to the plane of the interlaminar interface within the interface thickness and consequently enabling more effect of the filler on the interlaminar shear strength.

The flexural strength (Table 3) was increased by all three fillers (MWCNT, HHal and SiC whisker), such that the increase was greatest for MWCNT and least for SiC whisker. These results on flexural strength and short-beam shear strength mean that the increase in flexural strength upon HHal addition was at least partly due to an increase in the interlaminar shear strength, whereas the increase in flexural strength upon the addition of MWCNT or SiC whisker was essentially not due to an increase in the interlaminar shear strength, but was possibly due to the partial penetration of the laminae by the filler. This penetration is expected to be easier for MWCNT than SiC whisker, due to the relatively small size of MWCNT. As a consequence, the flexural strength enhancement was greater for MWCNT than SiC whisker.

4. Modeling

The calculation of the flexural modulus was based on the Rule of Mixtures, as explained below. This calculation required the volume fractions of the constituents. The volume fractions were obtained from the measured density of the composite and the Rule of Mixtures for the density (Table 1). The composite modulus values yielded the fiber modulus values (Table 5).

The modulus E_c of the unmodified unidirectional composite was given by
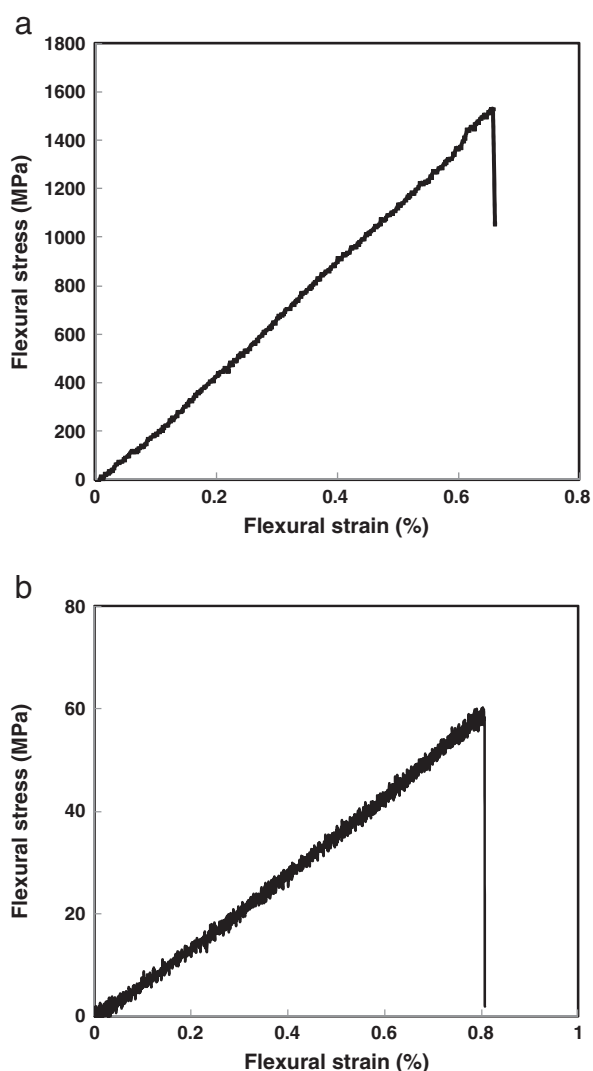
$$E_c = E_f v_f + E_m v_m, \tag{2}$$

where E_f and E_m were the moduli of the fiber and matrix respectively and v_f and v_m were the volume fractions of the fiber and matrix respectively. The values of E_m, as obtained from TenCate, was 3.48 GPa for the matrix. The composite modulus E_c was measured by static flexural testing in this work (Table 3 and Fig. 6). Thus, E_f was calculated by using Eq. (2), as shown in Table 5 for the longitudinal fiber modulus.

The modulus $E_c{}'$ of the modified unidirectional composite was given by

$$E_c{}' = E_f v_f{}' + E_m v_m{}' + E_{filler} v_{filler}, \tag{3}$$

where $v_f{}'$, $v_m{}'$, and v_{filler} were the volume fractions of the fiber, matrix and filler respectively, as obtained from the measured density values and the Rule of Mixtures for the density (Table 1). E_{filler} was the

Table 5
Measured and calculated values of the composite modulus of cross-ply carbon fiber epoxy composites fabricated at a curing pressure of 0.5 MPa.

Filler content[a]	Volume fraction			Fiber modulus (GPa)		Modulus (GPa)		Composite modulus (GPa)	
	Fiber	Matrix	Filler	0°	90°	Matrix	Filler	Calculated	Measured
0%	0.579	0.421	/	410	10.2	3.48	/	123.0	123.0
0.8% MWCNT	0.586	0.390	0.024	410	10.2	3.48	800	143.7	138.0 (124.5[b])
2% HHal	0.599	0.383	0.017	410	10.2	3.48	60	128.2	141.0 (127.2[b])
2% SiCw	0.593	0.393	0.014	410	10.2	3.48	550	133.7	137.0 (126.0[b])

[a] Fraction of mass of dispersion.
[b] Calculated value of the unmodified composite, obtained by scaling the measured value of the unmodified composite to the value for the higher fiber volume (Table 1) of the modified composite.

modulus of the fillers. The modulus values were taken as the following, in spite of the limited accuracy of available literature values: HHal (60 GPa (Lu et al., 2011)), SiC whisker (550 GPa (X. Zhang et al., 2009)), and MWCNT (800 GPa (Demczyk et al., 2002)).

The modulus E_c of the unmodified cross-ply composite was given by

$$E_c = E_f^{\ell}\left(\frac{v_f}{2}\right) + E_f^{t}\left(\frac{v_f}{2}\right) + E_m v_m, \qquad (4)$$

where E_f^{ℓ} and E_f^{t} were longitudinal fiber modulus and transverse fiber modulus respectively, v_f and v_m were the fiber and matrix volume fractions respectively, as obtained from the measured composite density values and the Rule of Mixtures for the density (Table 1), and E_c was measured by static flexural testing in this work (Table 3). The longitudinal fiber modulus E_f^{ℓ} of the unmodified cross-ply composite was calculated from Eq. (4).

The transverse fiber modulus E_f^t for the unmodified cross-ply composite was calculated by using the equation

$$E_c^{t} = E_f^{t} v_f + E_m v_m, \qquad (5)$$

where E_c^{t} was the transverse composite modulus, as measured in this work by static flexural texting of 90° unidirectional composites, and v_f and v_m were the same as the corresponding volume fractions of the 0° unidirectional composites.

The modulus $E_c^{'}$ of the modified cross-ply composite was given by

$$E_c^{'} = E_f^{\ell}\left(\frac{v_f^{'}}{2}\right) + E_f^{t}\left(\frac{v_f^{'}}{2}\right) + E_m v_m^{'} + E_{filler} v_{filler}, \qquad (6)$$

where $v_f^{'}$, $v_m^{'}$, and v_{filler} were the volume fractions of the fiber, matrix and filler respectively.

As shown in Table 5, there was reasonably good agreement between the corresponding calculated and measured composite modulus values, in spite of the limitations of the Rule of Mixtures and the inaccuracy of the values of the filler modulus. However, discrepancies were substantial. The model considered the filler volume fraction, but did not consider the interlaminar interface thickness.

The Rule of Mixtures model used in this work was adequate for showing that the observed increased in modulus and strength were in reasonable ranges. The modeling results were consistent with those of prior micromechanics modeling, which showed increases in modulus and strength due to carbon nanotube incorporation in glass fiber epoxy nanocomposites (Kim et al., 2010).

5. Conclusion

Heated low-cost natural Hal (0.1 μm diameter) were effective for strengthening and stiffening continuous carbon fiber polymer composites, as shown for cross-ply carbon fiber (5 μm diameter, ~59 vol.%) epoxy nanocomposites under flexure. Comparison was made among MWCNT, HHal and SiCw (with diameter 0.02, 0.1 and 1 μm respectively) in relation to the effectiveness for strengthening and stiffening the carbon fiber composite. Each filler was incorporated at the interlaminar interface by prepreg surface modification and amounted to ~2 vol.% of the composite.

The MWCNT was most effective, giving 25% increase in the strength, 11% increase in the modulus and 14% decrease in the ductility; HHal was almost as effective, giving 17% increase in the strength, 11% increase in the modulus and 21% decrease in the ductility; SiCw was slightly less effective, giving 15% increase in strength, 9% increase in modulus and 20% decrease in ductility. The flexural strength increase due to Hal nanotube incorporation corroborates with the interlaminar shear strength increase. However, the interlaminar shear strength was essentially not affected by the incorporation of MWCNT or SiCw. The measured values of the composite modulus agreed quite well with the calculated values based on the Rule of Mixtures.

For both modified and unmodified composites, the interlaminar interface thickness was below about 11 μm. The interlaminar interface thickness was higher for the SiC whisker case than the carbon nanotube or Hal nanotube case. The lamina thickness was not affected by the fillers. The composite density was 2% higher for the Hal nanotube and SiC whisker cases than the carbon nanotube case.

References

Alexopoulos, N.D., Bartholome, C., Poulin, P., Marioli-Riga, Z., 2010. Structural health monitoring of glass fiber reinforced composites using embedded carbon nanotube (CNT) fibers. Composites Science and Technology 70, 260–271.

Asi, O., 2009. Mechanical properties of glass-fiber reinforced epoxy composites filled with Al_2O_3 particles. Journal of Reinforced Plastics and Composites 28 (23), 2861–2867.

Bazhenov, S.L., 1995. Interlaminar and intralaminar fracture modes in 0/90 cross-ply glass/epoxy laminate. Composites 26, 125–133.

Bekyarova, E., Thostenson, E.T., Yu, A., Kim, H., Gao, J., Tang, J., Hahn, H.T., Choi, T., Itkis, M.E., Haddon, R.C., 2007. Multiscale carbon nanotube-carbon fiber reinforcement for advanced epoxy composites. Langmuir 23, 3970–3974.

Brigatti, M.F., Galan, E., Theng, B.K.G., 2006. In: Bergaya, F., Theng, B.K.G., Lagaly, G. (Eds.), Handbook of Clay Science. Elsevier, Oxford, UK, pp. 19–86.

Cho, J., Daniel, I.M., 2008. Reinforcement of carbon/epoxy composites with multi-wall carbon nanotubes and dispersion enhancing block copolymers. Scripta Materialia 58, 533–536.

Cho, J., Daniel, I.M., Dikin, D.A., 2008. Effects of carbon nanotube reinforcement on mechanical response and damage tolerance of carbon/epoxy composites. Proc. Am. Soc. Composites, Technical Conference, 23rd, pp. 89/1–89/14.

Chowdhury, F.H., Hosur, M.V., Jeelani, S., 2007. Investigations on the thermal and flexural properties of plain weave carbon/epoxy-nanoclay composites by hand-layup technique. Journal of Materials Science 42, 2690–2700.

Demczyk, B.G., Wang, Y.M., Cumings, J., Hetman, M., Han, W., Zettl, A., Ritchie, R.O., 2002. Direct mechanical measurement of the tensile strength and elastic modulus of multiwalled carbon nanotubes. Materials Science and Engineering A 334 (1–2), 173–178.

Du, M., Guo, B., Jia, D., 2010. Newly emerging applications of halloysite nanotubes: a review. Polymer International 59, 574–582.

Gao, L., Thostenson, E.T., Zhang, Z., Chou, T., 2009. Sensing of damage mechanisms in fiber-reinforced composites under cyclic loading using carbon nanotubes. Advanced Functional Materials 19, 123–130.

Godara, A., Gorbatikh, L., Kalinka, G., Warrier, A., Rochez, O., Mezzo, L., Luizi, F., van Vuure, A.W., Lomov, S.V., Verpoest, I., 2010. Interfacial shear strength of a glass fiber/epoxy bonding in composites modified with carbon nanotubes. Composites Science and Technology 70, 1346–1352.

Gojny, F.H., Wichmann, M.H.G., Fiedler, B., Bauhofer, W., Schulte, K., 2005. Influence of nano-modification on the mechanical and electrical properties of conventional fibre-reinforced composites. Composites Part A 36, 1525–1535.

Grimmer, C.S., Dharan, C.K.H., 2008. High-cycle fatigue of hybrid carbon nanotube/glass fiber/polymer composites. Journal of Materials Science 43, 4487–4492.

Grimmer, C.S., Dharan, C.K.H., 2010. Enhancement of delamination fatigue resistance in carbon nanotube reinforced glass fiber/polymer composites. Composites Science and Technology 70, 901–908.

Han, S., Lin, J.T., Aoyagi, Y., Chung, D.D.L., 2008. Enhancing the thermal conductivity and compressive modulus of carbon fiber polymer–matrix composites in the through-thickness direction by nanostructuring the interlaminar interface with carbon black. Carbon 46 (7), 1060–1071.

He, Y., Kong, W., Wang, W., Liu, T., Liu, Y., Gong, Q., Gao, J., 2012. Modified natural halloysite/potato starch composite films. Carbohydrate Polymers 87 (4), 2706–2711.

Hudnut, S.W., Chung, D.D.L., 1995. Use of submicron diameter carbon filaments for reinforcement between continuous carbon fiber layers in a polymer–matrix composite. Carbon 33 (11), 1627–1631.

Huertas, F.J., Fiore, S., Linares, J., 2004. In situ transformation of amorphous gels into spherical aggregates of kaolinite: a HRTEM study. Clay Minerals 39 (4), 423–431.

Hussain, M., Nakahira, A., Niihara, K., 1996. Mechanical property improvement of carbon fiber reinforced epoxy composites by Al_2O_3 filler dispersion. Materials Letters 26, 185–191.

Jia, Z., Luo, Y., Yang, S., Du, M., Guo, B., Jia, D., 2011. Styrene-butadiene rubber/halloysite nanotubes composites modified by epoxidized natural rubber. Journal of Nanoscience and Nanotechnology 11 (12), 10958–10962.

Kar, K.K., Rahaman, A., Agnihotri, P., Sathiyamoorthy, D., 2009. Synthesis of carbon nanotubes on the surface of carbon fiber/fabric by catalytic chemical vapor deposition and their characterization. Fullerenes, Nanotubes and Carbon Nanostructures 17, 209–229.

Kim, M., Park, Y., Okoli, O.I., Zhang, C., 2009. Processing, characterization, and modeling of carbon nanotube-reinforced multiscale composites. Composites Science and Technology 69, 335–342.

Kim, M., Mirza, F.A., Song, J.I., 2010. Micromechanics modeling for the stiffness and strength properties of glass fibers/CNTs/epoxy composites. WIT Transactions on the Built Environment 112, 279–290.

Kong, W., Wang, W., Gao, J., Liu, T., Liu, Y., 2011. Oxidized starch films reinforced with natural halloysite. Journal of Materials Research 26 (23), 2938–2944.

Lai, S., Chung, D.D.L., 1996. Consumption of SiC whiskers by the Al-SiC reaction in aluminum–matrix SiC whisker composites. Journal of Materials Chemistry 6 (3), 469–477.

Lecouvet, B., Sclavons, M., Bourbigot, S., Devaux, J., Bailly, C., 2011. Water-assisted extrusion as a novel processing route to prepare polypropylene/halloysite nanotube nanocomposites: structure and properties. Polymer 52 (19), 4284–4295.

Lee, O.H., Kim, S., Lim, Y., 2011. Conduction noise absorption by fiber-reinforced epoxy composites with carbon nanotubes. Journal of Magnetism and Magnetic Materials 323, 587–591.

Li, L., Chung, D.D.L., 1994. Thermally conducting polymer–matrix composites containing both AlN particles and SiC whiskers. Journal of Electronic Materials 23 (6), 557–564.

Lu, D., Chen, H., Wu, J., Chan, C.M., 2011. Direct measurements of Young's modulus of a single halloysite nanotube using a transmission electron microscope with a bending stage. Journal of Nanoscience and Nanotechnology 11, 7789–7793.

Rausch, J., Mader, E., 2010. Health monitoring in continuous glass fibre reinforced thermoplastics: manufacturing and application of interphase sensors based on carbon nanotubes. Composites Science and Technology 70, 1589–1596.

Rooj, S., Das, A., Heinrich, G., 2011. Tube-like natural halloysite/fluoroelastomer nanocomposites with simultaneous enhanced mechanical, dynamic mechanical and thermal properties. European Polymer Journal 47 (9), 1746–1755.

Segiet, M., Chung, D.D.L., 2000. Discontinuous surface-treated submicron-diameter carbon filaments as an interlaminar filler in carbon fiber polymer–matrix composites for vibration reduction. Composite Interfaces 7 (4), 257–276.

Sureeyatanapas, P., Young, R.J., 2009. SWNT composite coatings as a strain sensor on glass fibres in model epoxy composites. Composites Science and Technology 69, 1547–1552.

Thostenson, E.T., Li, W.Z., Wang, D.Z., Ren, Z.F., Chou, T.W., 2002. Carbon nanotube/carbon fiber hybrid multiscale composites. Journal of Applied Physics 91 (9), 6034–6037.

Thostenson, E.T., Gangloff Jr., J.J., Li, C., Byun, J., 2009. Electrical anisotropy in multiscale nanotube/fiber hybrid composites. Applied Physics Letters 95, 073111.

Timmerman, J.F., Hayes, B.S., Seferis, J.C., 2002. Nanoclay reinforcement effects on the cryogenic microcracking of carbon fiber/epoxy composites. Composites Science and Technology 62, 1249–1258.

Uddin, M.F., Sun, C.T., 2008. Impact resistance and toughness of composite laminates with nanoparticle-enhanced matrix. Int. SAMPE Symp. Exhib., vol. 53, pp. 354/1–354/11.

Wada, K., 1965. Intercalation of water in kaolin minerals. American Mineralogist 50 (7–8), 924–941.

Wang, S., Chung, D.D.L., 1997. Self-monitoring of strain in silicon carbide whisker reinforced silicon nitride. Smart Materials and Structures 6, 199–203.

Wang, S., Chung, D.D.L., 2006. Self-sensing of flexural strain and damage in carbon fiber polymer–matrix composite by electrical resistance measurement. Carbon 44 (13), 2739–2751.

Wang, W.X., Takao, Y., Matsubara, T., Kim, H.S., 2002. Improvement of the interlaminar fracture toughness of composite laminates by whisker reinforced interlamination. Composites Science and Technology 62, 767–774.

Ye, Y., Chen, H., Wu, J., Chan, C.M., 2011a. Interlaminar properties of carbon fiber composites with halloysite nanotubes-toughened epoxy matrix. Composites Science and Technology 71, 717–723.

Ye, Y., Chen, H., Wu, J., Chan, C.M., 2011b. Evaluation on the thermal and mechanical properties of HNT-toughened epoxy/carbon fibre composites. Composites: Part B 42, 2145–2150.

Yih, P., Chung, D.D.L., 1996. Silicon carbide whisker copper–matrix composites fabricated by hot pressing copper coated Whiskers. Journal of Materials Science 31, 399–406.

Yih, P., Chung, D.D.L., 1999. Brass–matrix silicon carbide whisker composites. Journal of Materials Science 34, 359–364.

Zhang, F., Wang, R., He, X., Wang, C., Ren, L., 2009. Interfacial shearing strength and reinforcing mechanisms of an epoxy composite reinforced using a carbon nanotube/carbon fiber hybrid. Journal of Materials Science 44, 3574–3577.

Zhang, X., Xu, L., Han, W., Weng, L., Han, J., Du, S., 2009. Microstructure and properties of silicon carbide whisker reinforced zirconium diboride ultra-high temperature ceramics. Solid State Sciences 11, 156–161.

Zhang, J., Zhuang, R., Liu, J., Mader, E., Heinrich, G., Gao, S., 2010. Functional interphases with multi-walled carbon nanotubes in glass fibre/epoxy composites. Carbon 48, 2273–2281.

Zhou, Y., Pervin, F., Rangari, V.K., Jeelani, S., 2006. Fabrication and evaluation of carbon nano fiber filled carbon/epoxy composite. Materials Science and Engineering A 426, 221–228.

Zhou, Y., Pervin, F., Jeelani, S., Mallick, P.K., 2008. Improvement in mechanical properties of carbon fabric-epoxy composite using carbon nanofibers. Journal of Materials Processing Technology 198, 445–453.

Zhu, J., Imam, A., Crane, R., Lozano, K., Khabashesku, V.N., Barrera, E.V., 2007. Processing a glass fiber reinforced vinyl ester composite with nanotube enhancement of interlaminar shear strength. Composites Science and Technology 67, 1509–1517.